Quantum Semiclass. Opt. **8** (1996) 931–938. Printed in the UK

Pattern selection in optical bistability

M Tlidi, R Lefever and Paul Mandel

Université Libre de Bruxelles, Campus Plaine, Code postal 231, 1050 Bruxelles, Belgium

Received 5 January 1996, in final form 26 March 1996

Abstract. Using the weakly nonlinear theory, we analyse the stability and relative stability of transverse patterns appearing in a passive Kerr cavity. We show that the hexagonal $H0$ structures are stable in the vicinity of the Turing bifurcation point. Numerical simulations confirm the analytical predictions.

1. Introduction

Optical bistability (OB) is a domain of nonlinear optics which has often been associated with optical processing. This has motivated much of the research on the topic and led to the necessary investigation of how transverse effects may modify the expected mode of operation of an optically bistable element. From a more fundamental viewpoint, the study of transverse effects in OB offers a challenge right from the derivation of the amplitude equations. Two models have been proposed, in two different limits. The first model, proposed by Lugiato and Lefever [1] (referred to as the LL model), describes OB in a medium with a cubic nonlinearity in the dispersive limit. The transverse effects appear via diffraction. The other model was proposed by Mandel *et al* [2] and describes OB in the double limit of nascent hysteresis and weak dispersion. In this second model, the transverse effects appear via a nonlinear diffusion equation of the Swift–Hohenberg type. This equation has been studied analytically in detail. A weakly nonlinear analysis and a relative stability analysis have been published [3, 4]. It turns out that the analytic work published on patterns and pattern selection in the LL model is less developed [5, 6]. It is the purpose of this paper to bridge this gap. Apart from the obvious interest in deriving analytic results for nonlinear partial differential equations, our analysis serves another purpose. It has recently been suggested that the spatially inhomogeneous solutions of the LL equation may not be stable close to the Turing instability [7]. It turns out that there is indeed a numerical problem when solving the LL equation in the long-time limit, but we have been able to match neatly the results of our analytic study with numerical solutions.

This paper is organized as follows. After briefly introducing the LL model, we present a derivation of the amplitude equations which admit stripes, rhomboids and hexagons as steady solutions. A linear analysis determines the domains of stability of these spatially inhomogeneous steady solutions. We find that there is an overlap between the domains of stability of the different solutions. Therefore, we perform a relative stability analysis to determine which of the patterns is more stable. Finally, we discuss some numerical simulations of the LL model in view of the different claims which have been published about the patterns' stability.

1355-5111/96/040931+08$19.50

2. The model

In the mean-field limit, the dynamics of the single longitudinal mode in the dispersive limit of the bistable system (cavity filled with a Kerr medium and driven by a coherent plane-wave field) can be described by the simple partial differential equation [1] (the LL model)

$$\frac{\partial x}{\partial t} = y - (1 + \mathrm{i}\theta)x + \mathrm{i}|x|^2 x + \mathrm{i}L_\perp x \tag{1}$$

which includes the effect of diffraction; x is the normalized slowly-varying envelope of the electric field, θ is the detuning parameter, y is the input field assumed to be real, positive and independent of the transverse coordinates and $L_\perp$ is the transverse Laplacian.

The homogeneous stationary solutions of (1), $\bar{x}$, are given by

$$y^2 = |\bar{x}|^2[1 + (\theta - |\bar{x}|^2)^2]\,. \tag{2}$$

For $\theta < \sqrt{3}$ ($\theta > \sqrt{3}$) the transmitted intensity as a function of the input intensity y^2 is monostable (bistable).

The homogeneous steady state $\bar{x}$ undergoes a Turing bifurcation at

$$y_c^2 = 1 + (1 - \theta)^2 \qquad |\bar{x}|_c^2 = 1\,. \tag{3}$$

At this bifurcation point, the critical wavenumber is $k_c^2 = 2 - \theta$.

3. Weakly nonlinear analysis

3.1. Derivation of the amplitude equations

In this section we shall describe the nonlinear evolution of the system in the vicinity of the instability point y_c. The small-amplitude inhomogeneous stationary solutions (stripes, hexagons, rhomboids) can be calculated analytically by employing the standard theory [8]. For this purpose we first decompose the electric field into its real and imaginary parts:

$$x = x_1 + \mathrm{i}x_2 \tag{4}$$

and introduce the excess variables u and v:

$$x_1(\boldsymbol{r}, t) = \bar{x}_1 + u(\boldsymbol{r}, t) \tag{5}$$

$$x_2(\boldsymbol{r}, t) = \bar{x}_2 + v(\boldsymbol{r}, t) \tag{6}$$

where $\boldsymbol{r}$ denotes the transverse coordinates and $\bar{x}_1$ and $\bar{x}_2$ are, respectively, the real and imaginary parts of the homogeneous stationary solution (1) given by

$$-\bar{x}_1 + y - \bar{x}_2(\bar{x}_1^2 + \bar{x}_2^2 - \theta) = 0 \tag{7}$$

$$-\bar{x}_2 + \bar{x}_1(\bar{x}_1^2 + \bar{x}_2^2 - \theta) = 0\,. \tag{8}$$

By solving equations (7) and (8) and using (3), the critical values of $\bar{x}_1$, $\bar{x}_2$ are found to be $\bar{x}_{1c} = 1/y_c$ and $\bar{x}_{2c} = (1 - \theta)/y_c$.

Inserting (4)–(6) into the LL model and using (7), (8), we obtain the following equations:

$$\frac{\partial u}{\partial t} = (-1 - 2\bar{x}_1\bar{x}_2)u + [-(3\bar{x}_2^2 + \bar{x}_1^2 - \theta) - L_\perp]v$$
$$-[\bar{x}_2 u^2 + 2\bar{x}_1 uv + 3\bar{x}_2 v^2 + u^2 v + v^3] \tag{9}$$

$$\frac{\partial v}{\partial t} = (3\bar{x}_1^2 + \bar{x}_2^2 - \theta + L_\perp)u + (-1 + 2\bar{x}_1\bar{x}_2)v$$
$$+[3\bar{x}_1 u^2 + 2\bar{x}_2 uv + \bar{x}_1 v^2 + uv^2 + u^3]\,. \tag{10}$$

Next, we introduce a smallness parameter $\varepsilon \ll 1$ which measures the distance from the critical point, and expand the input field amplitude y and all variables u, v, $\bar{x}_1$ and $\bar{x}_2$ around their critical values at the bifurcation point:

$$y = y_c + \varepsilon p_1 + \varepsilon^2 p_2 + \cdots \tag{11}$$

$$u = \varepsilon[u_0(\boldsymbol{r}, \tau) + \varepsilon u_1(\boldsymbol{r}, \tau) + \varepsilon^2 u_2(\boldsymbol{r}, \tau) + \cdots] \tag{12}$$

$$v = \varepsilon[v_0(\boldsymbol{r}, \tau) + \varepsilon v_1(\boldsymbol{r}, \tau) + \varepsilon^2 v_2(\boldsymbol{r}, \tau) + \cdots] \tag{13}$$

$$\bar{x}_1 = \bar{x}_{1c} + \varepsilon a_1 + \varepsilon^2 a_2 + \cdots \tag{14}$$

$$\bar{x}_2 = \bar{x}_{2c} + \varepsilon b_1 + \varepsilon^2 b_2 + \cdots \tag{15}$$

and also introduce the slow time $\tau = \varepsilon^2 t$.

Near the critical point we can approximate the solution to leading order in ε as a linear superposition of the corresponding critical modes k_i:

$$(u_0, v_0) = \left(1, \frac{1+\rho}{1-\rho}\right) \sum_{j=1}^{l} [\bar{W}_j \exp \mathrm{i}(\boldsymbol{k}_j \cdot \boldsymbol{r}) + \mathrm{CC}] \qquad \text{with} \quad |\boldsymbol{k}_j| = k_c \tag{16}$$

where CC denotes the complex conjugate and $\rho = 1 - \theta$. The stripes and the rhomboids are characterized by $l = 1$ and 2, respectively, and the hexagons are obtained for $l = 3$ with $\boldsymbol{k}_1 + \boldsymbol{k}_2 + \boldsymbol{k}_3 = \boldsymbol{0}$. Note that the complex amplitude $\bar{W}_j$ associated with the mode k_j depends only on the slow time τ.

The quantities a_i, b_i, u_i and v_i ($i = 1, 2$) can be calculated by inserting (11)–(15) into (7)–(10) and equating terms with the same powers of ε. The coefficients are given in [9]. The application of the solvability condition to the higher-order inhomogeneous problem leads to a set of amplitude equations for the unstable mode. In terms of the unscaled amplitudes ($W_i = \varepsilon \bar{W}_i + \cdots$, with $i = 1, 2, 3$), we have, for the stripes

$$\frac{1}{2y_c^2} \frac{\partial W_1}{\partial t} = \mu W_1 - g_1(\rho) W_1 |W_1|^2 \tag{17}$$

where

$$\mu = \frac{(y - y_c)}{y_c(1+\rho)^2} \tag{18}$$

$$g_1(\rho) = \frac{2(30\rho + 11)}{9(1-\rho^2)^2}\,. \tag{19}$$

If we introduce the polar decomposition $W_1 = A_1 \exp(\mathrm{i}\phi_1)$, we see that the phase ϕ_1 is arbitrary and the real stationary amplitudes of the stripes are given by $A_{S0} = 0$ or $A_{S\pm} = \pm\sqrt{\mu / g_1(\rho)}$. The linear stability analysis of these stationary solutions shows that if $g_1(\rho) < 0$, the trivial solution A_{S0} remains stable for $y < y_c$, while the inhomogeneous solution is stable for $y > y_c$, i.e. it appears supercritically.

For the rhomboids, we obtain

$$\frac{1}{2y_c^2} \frac{\partial W_1}{\partial t} = \mu W_1 - g_1(\rho) W_1 |W_1|^2 - g_2(\rho, \beta) W_1 |W_2|^2 \tag{20}$$

where

$$g_2(\rho, \beta) = \frac{8[(2\rho+1)(1 - 16\cos^4\beta) + 4]}{(1-\rho^2)^2(1 - 4\cos^2\beta)^2} \tag{21}$$

with β being the angle between $\boldsymbol{k}_1$ and $\boldsymbol{k}_2$. The amplitude equation for W_2 is obtained from (20) by permutation of indices. By setting $W_j = A_j \exp(\mathrm{i}\phi_j)$ in equation (20), we obtain

that the phases are arbitrary and the real stationary amplitudes of the rhomboid patterns read as $A_{R\pm} = \pm\sqrt{-\mu/(g_2 - g_1)}$, which exist if $g_2(\rho, \beta) - g_1(\rho) < 0$ and are stable if

$$g_2(\rho, \beta) + g_1(\rho) < 0\,. \tag{22}$$

For hexagons, the amplitude equations are

$$\frac{1}{2y_c^2}\frac{\partial W_1}{\partial t} = \mu W_1 - g_1 W_1|W_1|^2 + h_1(|W_2|^2 + |W_3|^2)W_1 + h_2 W_2^\star W_3^\star \tag{23}$$

where

$$h_1(\rho) = \frac{1 - 4\rho}{(1-\rho^2)^2}$$

$$h_2(\rho) = \frac{1}{y_c(1-\rho)} + F(\rho)(y - y_c)/y_c$$

$$F(\rho) = \frac{3\rho^4 + 16\rho^3 + 14\rho^2 + 16\rho + 7}{2(1+\rho)^4(1-\rho)(1+\rho^2)}\,.$$

The evolution equations for W_2 and W_3 are obtained by a cyclic permutation of the indices. Note that the coefficient of the quadratic term in (23) depends on $(y - y_c)/y_c$. This is due to the fact that the coefficient $F(\rho)$ is relatively large. In this case we have to include the renormalization term proportional to the relative distance from the bifurcation point [10, 11]. In the following discussion, we consider $g_1(\rho) > 0$ and $h_1(\rho) < 0$. These two conditions restrict the analysis to the values of detuning parameter ($\theta = 1 - \rho$) in the range

$$\theta < \tfrac{3}{4} \tag{24}$$

in which the homogeneous steady state is necessarily monostable.

To determine the stationary hexagonal solutions we employ the method which we used for stripes and rhomboids. The steady state solutions for the phases and amplitudes are given by

$$\sin\psi_s = 0 \qquad \text{with} \quad \psi_s = \phi_1 + \phi_2 + \phi_3 \tag{25}$$

$$A_{H\pm} = \frac{-h_2\cos\psi_s \pm \sqrt{h_2^2 - 4\mu(2h_1 - g_1)}}{2(2h_1 - g_1)}\,. \tag{26}$$

There are two types of stationary hexagonal patterns: $H0$ corresponding to $\psi_s = 0$ and $H\pi$ corresponding to $\psi_s = \pi$. The domains of their stability are mutually exclusive: the $H0$'s ($H\pi$) are stable (unstable) for $h_2 < 0$ ($h_2 > 0$). Here, the coefficient h_2 of the quadratic term in (23) is always positive. Then, in the vicinity of the instability point y_c, the hexagonals $H\pi$ ($H0$) are unstable (stable).

3.2. Pattern competition

The preceding analysis has shown the existence and stability of different periodic solutions. In order to ascertain which one will be selected by the system, we must perform a relative stability analysis, i.e. the stability of one pattern to perturbations favouring another pattern.

Let us start by studying the rhomboid–stripe competition. We perturb the stripes' amplitude solution $A_{S\pm} = \pm\sqrt{\mu/g_1(\rho)}$ by a small perturbation with rhomboid symmetry: $A_1 = A_S + u$, $A_2 = v$ with $u, v \ll 1$. We substitute these relations into the real part of the amplitude equations (20) associated to the rhomboid patterns and linearize to obtain

$$\frac{1}{2y_c^2}\frac{\partial u}{\partial t} = -2\mu u \qquad \frac{1}{2y_c^2}\frac{\partial v}{\partial t} = \mu\left[1 + \frac{g_2(\rho,\beta)}{g_1(\rho)}\right]v\,. \tag{27}$$

From equation (27) we deduce the condition under which the stripes are stable for $y > y_c$: $g_2(\rho, \beta) + g_1(\rho) > 0$. This condition is incompatible with (22). We conclude that the rhomboids are always unstable in the LL model close to the Turing bifurcation.

Let us now consider the hexagon–stripe competition. We add to the stripes' amplitudes $A_{S\pm} = \pm\sqrt{\mu/g_1(\rho)}$ a small perturbation with hexagonal symmetry: $A_1 = A_{S\pm} + u$, $A_2 = v$ and $A_3 = w$ with $u, v, w \ll 1$. We replace these relations in the real part of (23) and linearize to obtain

$$\frac{1}{2y_c^2}\frac{\partial u}{\partial t} = -2\mu u \qquad \frac{1}{2y_c^2}\frac{\partial v}{\partial t} = cv + c'w \qquad \frac{1}{2y_c^2}\frac{\partial w}{\partial t} = c'v + cw$$

where $c = \mu\left[1 + h_1(\rho)/g_1(\rho)\right]$ and $c' = h_2(\rho)A_{S\pm}$.

If $y > y_c$, u decreases to zero reflecting the fact that the stripes are stable with respect to a perturbation which affects only the amplitude A_1. The roots of the characteristic equation which governs the stability for the perturbation u and v are given by $\lambda^{\pm} = 2y_c^2(c \pm c')$. In the range given by (24), λ^+ is always positive. This implies that the stripes are never stable and the stripe–hexagon transition is therefore not observed in this model. Such a transition has been observed in nascent optical bistability [3, 4], where the dynamics is governed by the Swift–Hohenberg equation [2]. This type of transition was also observed in the numerical studies of the absorptive system [12].

The results of the stability and the relative stability analyses are summarized in the bifurcation diagram (cf figure 1). We plot the amplitude of stripes, hexagons $H0$ and $H\pi$ versus the relative distance from the Turing bifurcation point $(y - y_c)/y_c$ for the detuning parameter $\theta = 0.7$, i.e. $\rho = 0.3$. We can see that both stripes and hexagons $H\pi$ appear supercritically. On the other hand, the solution A_{H-} (see equation (26) with $\psi_s = 0$) associated to the hexagons $H0$ emerges subcritically from the homogeneous solution at the bifurcation point and is unstable until it reaches a limit point given by $h_2^2 = 4\mu(2h_1 - g_1)$, from which the branch A_{H+} emerges and is stable.

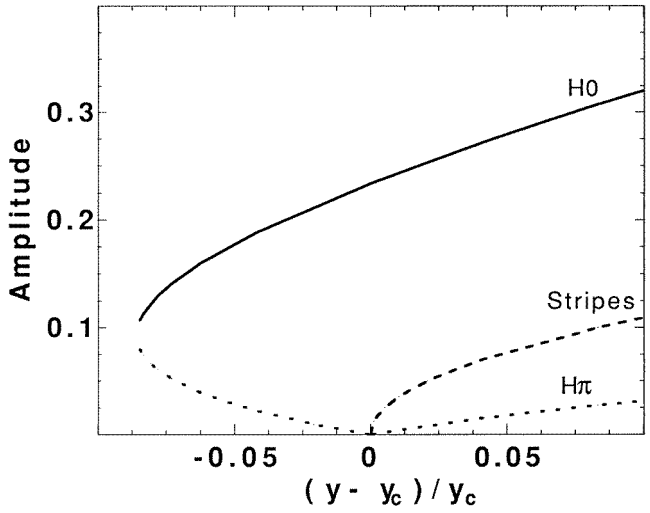

Figure 1. Bifurcation diagram ($\theta = 0.7$). The full and broken lines correspond, respectively, to the stable and unstable inhomogeneous solutions.

4. Numerical simulations and conclusions

We have developed two numerical methods to integrate the LL model (1) in two transverse dimensions with periodic boundary conditions: one is a pure implicit method [3], the other is the odd–even hopscotch method [13, 14]. To make explicit comparisons with our analytical results, the numerical solutions are obtained for the parameter range where the system exhibits a monostable homogeneous steady state solution. We fix the detuning parameter at $\theta = 0.7$ and vary the input field intensity y^2. In this case, the transverse instability occurs at $y_c \approx 1.044$ (see equations (3)). The grid used for our simulation is 128×128 and the choice of the initial conditions depends on the parameter range; for $y > y_c$ we perturb the homogeneous steady state by the small random noise, and for $y < y_c$ we use small amplitude patterns of different symmetry. For $y = 0.98$ we observe a stable hexagonal structure (cf figure 2). Above the instability point, for $y = 1.05$ which means $(y - y_c)/y_c = 0.0057$, the hexagonal structure is stable. In figure 3, we show how the system evolves from the unstable homogeneous state towards the stable inhomogeneous state. Note that the transition between the two states is abrupt, but takes place after a fairly long transient close to the homogeneous state.

To compare with the analytical results, we first calculate the wavelength ($\Lambda_{th} = 2\pi/k_c = 2\pi/\sqrt{2-\theta} \approx 5.51$) given by the linear stability analysis and that of the stable hexagonal structure obtained numerically ($\Lambda_{num} \approx 5.82$). We see a very good agreement with the two wavelengths. Next, we compare the two amplitudes obtained by analytical calculation and by simulation. This is displayed in figure 4. We can see that near the limit point the

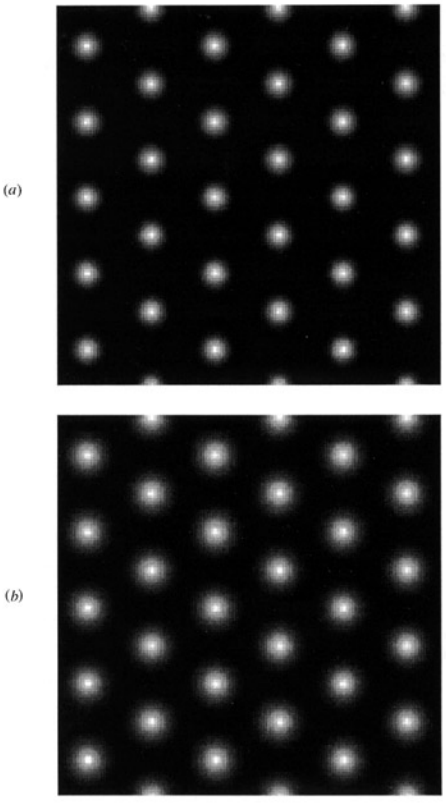

Figure 2. Hexagonal structure in the monostable case. Parameters are $y = 0.98$ and $\theta = 0.7$. Maxima are plain white. (*a*) Real part of the electric field. (*b*) Imaginary part.

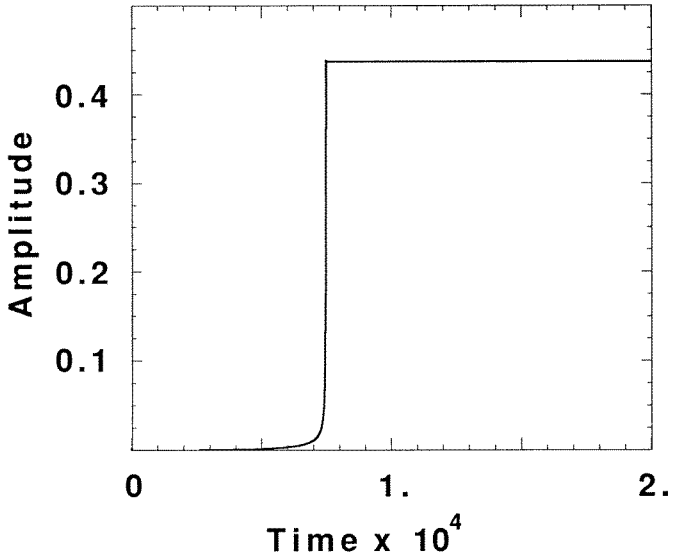

Figure 3. Difference between the maximum and minimum hexagonal amplitude corresponding to the real part of the electric field. Parameters are $y = 1.05$ and $\theta = 0.7$. The time step is 3.125×10^{-3}.

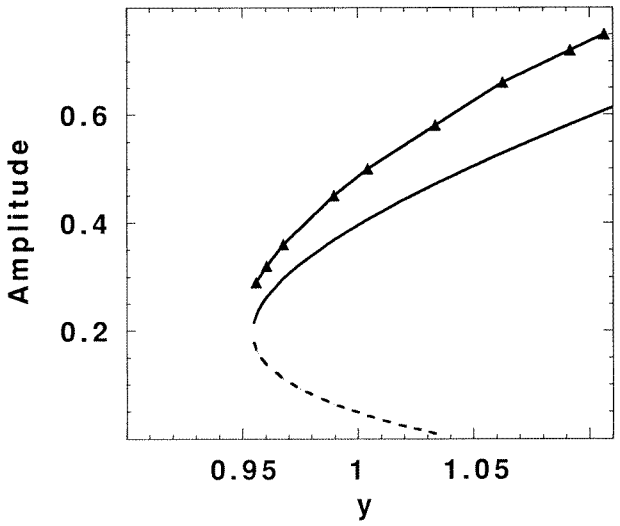

Figure 4. Bifurcation diagram in two transverse dimensions ($\theta = 0.7$). The full and the broken curve indicate, respectively, stable and unstable theoretical amplitude of electric field. The triangles indicate the corresponding intensity obtained by numerical simulations.

comparison is good, but far from this point the numerical amplitude becomes larger than that obtained by simulation.

Acknowledgments

This work was supported in part by the Fonds National de la Recherche Scientifique (Belgium) and the inter-university Attraction Pole program of the Belgian government.

References

[1] Lugiato L A and Lefever R 1987 *Phys. Rev. Lett.* **58** 2209
[2] Mandel P, Georgiou M and Erneux T 1993 *Phys. Rev.* A **47** 4277
[3] Tlidi M, Georgiou M and Mandel P 1993 *Phys. Rev.* A **48** 4605
[4] Tlidi M and Mandel P 1994 *Chaos Solitons Fractals* **4** 1475
[5] Firth W F, Scroggie A J, McDonald G S and Lugiato L A 1992 *Phys. Rev.* A **46** 3609
[6] Scroggie A J, Firth W F, McDonald G S, Tlidi M, Lefever R and Lugiato L A 1994 *Chaos Solitons Fractals* **4** 1323
[7] Le Berre M, Ressayre E and Tallet A 1994 *Quantum Semiclass. Opt.* **7** 1
[8] Manneville P 1990 *Dissipative Structures and Weak Turbulance* (New York: Academic)
[9] Tlidi M 1995 *PhD Thesis* ULB Belgium, unpublished
[10] Pismen L M 1986 *Chemical Engineering: Concepts and Reviews* ed V H Hlavacek (New York: Gordon and Breach)
[11] Verdasca J, De Wit A, Dewel G and Borckmans P 1992 *Phys. Lett.* **168A** 194
[12] Firth W F and Scroggie A J 1994 *Europhy. Lett.* **26** 521
[13] Gourlay A R 1970 *J. Inst. Math. Appl.* **6** 423
[14] Hardin R H and Flannery B P 1973 *SIAM Rev.* **15** 986